Characterisation of hepcidin response to holotransferrin treatment in CHO TRVb-1 cells

Patel, V. B., Mehta, K., Greenwell, P., Renshaw, D., Busbridge, Mark, Garcia, M and Farnaud, S.

Characterisation of hepcidin response to holotransferrin treatment in CHO TRVb-1 cells

Kosha Mehta[1], Pamela Greenwell[1], Derek Renshaw[1], Mark Busbridge[2], Mitla Garcia[3], Sebastien Farnaud[4*] and Vinood B. Patel[1*]

[1]Department of Biomedical Sciences, University of Westminster, London W1W 6UW, UK
[2]Department of Clinical Biochemistry, Charing Cross Hospital, Imperial College Healthcare NHS Trust, London W6 8RF, UK
[3]Randall Division of Cell and Molecular Biophysics, King's College London SE1 1UL, UK
[4]Department of Life Sciences, University of Bedfordshire, Luton, LU1 3JU, UK
*Equal contribution

Corresponding author: Dr Vinood Patel, Department of Biomedical Sciences, Faculty of Science and Technology, University of Westminster, London W1W 6UW, UK. Email: v.b.patel@westminster.ac.uk, Tel 0207 911 5000 ext. 64138.

Abstract

Iron overload coupled with low hepcidin levels are characteristics of hereditary haemochromatosis. To understand the role of transferrin receptor (TFR) and intracellular iron in hepcidin secretion Chinese hamster ovary transferrin receptor variant (CHO TRVb-1) cells were used that express iron-response-element-depleted human *TFRC* mRNA (TFRCΔIRE). Results showed that CHO TRVb-1 cells expressed higher basal levels of cell-surface TFR1 than HepG2 cells (2.2-fold; $p<0.01$) and following 5 g/L holotransferrin treatment maintained constitutive over-expression at 24 h and 48 h, contrasting the HepG2 cells where the receptor levels significantly declined. Despite this, the intracellular iron content was neither higher than HepG2 cells nor increased over time under basal or holotransferrin-treated conditions. Interestingly, hepcidin secretion in CHO TRVb-1 cells exceeded basal levels at all time-points ($p<0.02$) and matched levels in HepG2 cells following treatment. While *TFRC* mRNA expression showed expected elevation (2 h, $p<0.03$; 4 h; $p<0.05$), *slc40a1* mRNA expression was also elevated (2 h, $p<0.05$; 4 h, $p<0.03$), unlike the HepG2 cells. In conclusion, the CHO TRVb-1 cells prevented cellular iron-overload by elevating *slc40a1* expression, thereby highlighting its significance in the absence of iron-regulated *TFRC* mRNA. Furthermore, hepcidin response to holotransferrin treatment was similar to HepG2 cells and resembled the human response.

Keywords: hepcidin, iron regulation, iron response element, transferrin receptor

Introduction

Hepcidin is a liver-secreted, 25-mer peptide hormone responsible for maintaining iron homeostasis in the body [1]. Systemic iron elevation leads to increased levels of hepcidin that binds to ferroportin, the cellular iron-exporter, and induces internalisation and degradation of both hepcidin and ferroportin [2]. Thereby, it prevents cellular iron-efflux and regulates systemic iron levels. However, the iron-sensing mechanisms that lead to hepcidin secretion are unclear. A putative role of transferrin receptor (TFR)1 in modulating hepcidin expression was suggested [3] but its significance in transferrin-sensing and hepcidin induction has not been sufficiently emphasised. Likewise, even though an involvement of intracellular iron in the maturation of prohepcidin into bioactive hepcidin was postulated [4], its function in hepcidin peptide secretion has not been sufficiently examined. This is partly because of lack of suitable cell lines that could consistently mimic the human hepcidin response to iron treatments. Also, majority of previous *ex vivo* iron supplementation studies and even some current investigations focussed on transcriptional regulation of hepcidin [5] and not on bioactive hepcidin peptide.

These issues have been addressed in the present study where holotransferrin (holo-Tf) induced hepcidin peptide secretion was examined in Chinese hamster ovary transferrin receptor variant (CHO TRVb-1) cells. These cells lack endogenous TfR1 and express iron response element (IRE)-depleted human *TFRC* mRNA (*TFRC*ΔIRE) [6]. Due to this unique feature it was hypothesised that upon holo-Tf treatment, these cells would bypass the IRE-dependent *TFRC* mRNA regulation by iron [7] and show increased iron-uptake. The effect of this on hepcidin secretion could be studied and compared with HepG2 cells that possess iron-regulated *TFRC* mRNA. Accordingly, after defining the iron saturation of the iron source and iron content of the treatment medium, the effect of holo-Tf treatment on cell-surface TFR1, intracellular iron content and hepcidin secretion were studied over short and long time-periods. Furthermore, mRNA expression of CHO-endogenous *slc40a1* and human *TFRC* was examined under holo-Tf excess to further understand cellular iron regulation in the absence of iron-regulated *TFRC*. To enable this, the previously unknown sequence of s*lc40a1* in the CHO TRVb-1 cells was characterised.

Materials and Methods

Cell culture

Wild type (Wt) CHO and CHO TRVb-1 clone B6, donated by Professor Keith Caldecott (University of Sussex, UK) and Dr. Heinz Zoller (University of Innsbruck, Austria), respectively, were maintained in Ham's F12 nutrient mixture (1X) (Invitrogen, UK) with 2 mM glutamax (Fisher Scientific,UK), 10 % foetal calf serum (FCS) (Biosera, UK) and 1 % antibiotic/antimycotic solution (100X) (Fisher Scientific, UK). HepG2 cells (Health Protection Agency, UK) were maintained in Eagle's Minimum Essential Medium (EMEM) (Sigma-Aldrich, UK).

Iron treatment studies

Apo-Tf was iron-loaded using 0.1 M ferric citrate and iron saturation of 5 g/L holo-Tf was confirmed by polyacrylamide gel electrophoresis using a 6 M urea gel [8]. Iron concentration in holo-Tf treatment medium was determined by ferrozine assay [9]. Cells were seeded at a density of 5 X 10^5 cells in a 6-well plate and maintained until 60 % - 70 % confluent. After washing with phosphate buffered saline (PBS) (Invitrogen, UK), cells were treated with serum-free EMEM (0 g/L) or 5 g/L holo-Tf from 30 minutes (min) to 24 h and various parameters were assessed, as described below.

Detection of human transferrin receptor at mRNA and protein levels in CHO TRVb-1 cells

To detect *TFRC* transcripts in CHO cells, PCRs were conducted with cDNA as template and primers listed in the succeeding section. Human TFR1 protein in the CHO TRVb-1 cells was confirmed by immunoblotting. Cell pellet was mixed with 2X Laemmli buffer and loaded on 10 % SDS gels (BIO-RAD, UK.) After electrophoresis, proteins were transferred to a PVDF membrane and blocked with 10 % fat-free milk in PBS for 1 h at room temperature (RT). Membranes were probed with primary human TFR1 antibody 3B82A1 (Thermo scientific, UK) [1:2000] for 1 h at RT and then incubated with a rabbit anti-mouse HRP-conjugated secondary antibody (Dako Ltd, UK) [1:1000] for 1 h at RT. Bands were visualised using ECL™ Western Blotting Detection Reagents (GE healthcare, UK) on X-ray film.

For analysis of cell-surface TFR1 expression, cells were harvested using TrypLE Express (ThermoFisher Scientific, UK), followed by centrifugation for 4 min at 89 x *g*. Cells were suspended in PBC (PBS containing 0.15 % BSA and 1 mM calcium chloride) and transferred

to a 96-well plate (2 X 10^5 cells per well) and centrifuged at 1,260 x *g* for 30 sec. To each well, 20 µL of 16 mg/mL blocking IgG was added. Human transferrin receptor antibody (Abcam, UK) [5 µg/mL in PBC)] was added to each test well and PBC was added to the control wells. Cells were incubated for 45 min on ice. Following washing, the cells were incubated with 10 µg/mL of FITC-labelled secondary antibody STAR9B rabbit F (ab')2 anti-mouse IgG (ABD Serotec, UK). After incubation for 30 min on ice, cells were washed with PBC again. Cell layer at the bottom of each well was resuspended in 400 µL of PBS and TFR1 expression was analysed by flow cytometry [10].

Determination of intracellular iron content and hepcidin peptide levels and mitochondrial activity

Cellular iron content, as determined by the ferrozine assay [9], was expressed as nmoles of iron per mg of protein, as quantified by the Bradford method. The ferrozine assay can detect levels from 2 to 300 µM and compares favourably to atomic absorption spectroscopy [9] and and ICP-MS [11]. The concentration of hepcidin peptide secreted in the cell media was measured as described by Busbridge et.al [12]. Here, using a rabbit anti-human hepcidin antibody, plasma hepcidin range from 1.1–55 ng/mL, with a median of 10.8 ng/mL in healthy controls, while the limit of detection is 0.6 ng/mL and linearity is up to 200 ng/mL [12]. The mitochondrial activity was assessed using the MTT assay [13].

Primer design, cDNA synthesis, sequencing and gene expression analyses

Primers were designed through software *Primer 3* (*http://frodo.wi.mit.edu/)*. Primers CCCAGCAGAAGCATTATCTTT (F) and TTCCCATCAATTGGATGTCTT (R) for CHO-endogenous *TfRC* and AAAATCCGGTGTAGGCACAG (F) and TTAAATGCAGGGACGAAAGG (R) for human *TFRC* were used to detect *TFRC* transcripts in CHO cells. For gene expression analyses, the primers AAAATCCGGTGTAGGCACAG (F) and TTAAATGCAGGGACGAAAGG (R) for human *TFRC*, ATGGGTGCTCACTGTCTGCTA (F) and GCATTCATATCTGCTAATCTGCTTC (R) for CHO-*slc40a1*, GCTCTTTTCCAGCCTTCCTT (F) and GAGCCAGAGCAGTGATCTCC (R) for CHO- *beta-actin* [14], TGTTTCTGGTAGAGCTCTAT (F) and GATATAGCAGGAAGTGAGAA (R) for human *SLC40A1* and GCCAAAAGGGTCATCATCTC (F) and GGTGCTAAGCAGTTGGTGGT (R) for *GAPDH* [15] were used. RNA was extracted using the TRI reagent (Sigma-Aldrich, UK), reverse transcription and cDNA synthesis was performed using QuantiTect reverse

transcription kit (Qiagen, UK) and PCRs were performed using Taq PCR master mix (Qiagen, UK). All PCR products were sequenced to confirm product identity. Prior to sequencing, amplicons were electrophoresed on 1 % agarose gel (Web Scientific, UK) to confirm product size and purified using PCR product purification kit (Qiagen, UK). Sequencing was conducted at the Wolfson Institute for Biomedical Research (University College London, UK). Gene expression was analysed through real-time PCR using Qiagen's Quantifast SYBR green kit in Rotor-gene Q machine (Qiagen, UK) and results were analysed using Rotor-gene software series 1.7. Data was expressed as $2^{-\Delta\Delta Ct}$ [16].

Characterisation of s*lc40a1* sequence in CHO TRVb-1 cells

DNA was extracted using the isopropanol-ethanol precipitation method [17]. To characterise the previously unknown s*lc40a1* sequence in CHO TRVb-1 cells, genomic similarities between related species were assessed (supplementary Table 1) and "PCR walking" was used (supplementary information). Characterised CHO-s*lc40a1* gene sequence was translated to its protein sequence (referred as CHO-ferroportin) by using the *TRANSLATE* tool (*http://web.expasy.org/translate*) and compared with ferroportin sequences of human, mouse and rat (supplementary Table 2) by using *ClustalW2* (*www.ebi.ac.uk*).

Bioinformatics analysis of hepcidin peptide sequences

To assess peptide sequence similarities between human and Chinese hamster, multiple sequence alignments were created via *CLUSTAL O* (1.2.1) available via UniProtKB (supplementary Table 2).

Statistical analysis

Data was analysed by using one-way or two-way ANOVA, accompanied by post-hoc analysis by Tukey's test using the software SPSS, version 19. The level of significance was set at $p<0.05$.

Results

Characterisation of CHO TRVb1-cells in basal conditions

TFR1 expression: Presence of human *TFRC* mRNA and absence of CHO-endogenous *Tfrc* mRNA in CHO TRVb-1 cells was confirmed (Fig.1a). Here, only wt CHO cDNA formed product with primers for CHO-endogenous *Tfrc* (lane 1). As expected, CHO TRVb-1 cDNA did not form product with primers for CHO-endogenous *Tfrc* but formed

product with primers for human *TFRC* (lanes 3 and 4, respectively). Human TFR1 protein in the CHO TRVb-1 cells showed expected bands of approximately 180 kDa (lane 1) and 85-90 kDa (lane 2) under non-reducing and reducing conditions, respectively (Fig.1b), as previously observed [18]. Also, the CHO-TRVb1 cells showed significantly higher levels of cell-surface TFR1 than HepG2 cells (2.2-fold; $p<0.01$) (Fig.1c).

Intracellular iron content and hepcidin secretion: Under basal conditions, CHO TRVb-1 cells maintained intracellular iron content over time and did not differ significantly from HepG2 cells (Fig.2a). Hepcidin secretion in CHO TRVb-1 cells declined over time from 30 min to 2 h ($p<0.05$), followed by substantial reduction at 24 h (3.6-fold; $p<0.01$), while the HepG2 cells showed constant hepcidin levels (Fig.2b). The CHO TRVb-1 cells secreted significantly lower levels of hepcidin than HepG2 cells at 2 h ($p<0.04$) and 24 h ($p<0.02$).

Iron supplementation studies in CHO TRVb-1 cells

Analysis of iron saturation of holo-Tf indicated that 90 % of the protein was diferric, with a minor proportion of monoferric transferrins (supplementary Fig.2a). Also, iron content in 5 g/L holo-Tf treatment medium was determined as 105 µM, which was 84 % of the expected iron molarity of 125 µM in a 5 g/L holo-Tf preparation (supplementary Fig.2b).

Cell-surface TFR1 expression: Upon 5 g/L holo-Tf treatment, the CHO TRVb-1 cells maintained elevated TFR1 expression at 48 h, contrasting the HepG2 cells where TFR1 levels significantly declined from 24 h to 48 h ($p<0.01$) (Fig.3).

Intracellular iron content: Following holo-Tf deprivation (0 g/L), the CHO TRVb-1 cells neither showed significant variation in intracellular iron content over time nor differed in iron content from the HepG2 cells (Fig.4a). Upon holo-Tf treatment (5 g/L), the CHO TRVb-1 cells showed significantly reduced intracellular iron content from 30 min to 4 h (2.2-fold; $p<0.01$) (Fig.4b). However, the levels significantly increased from 4 h to 24 h ($p<0.05$) and restored iron levels to that observed at earlier time points. Iron levels did not majorly differ from the HepG2 cells, except at 4 h ($p<0.02$) (Fig.4b).

Hepcidin levels: Holo-Tf deprivation in CHO TRVb-1 cells (Fig.4c) caused a significant decline in hepcidin secretion over time from 30 min to 24 h (2.8-fold; $p<0.01$). The levels were similar to HepG2 cells, except at 4 h where the levels in CHO TRVb-1 cells were higher than levels in HepG2 cells (1.9-fold; $p<0.02$). Upon holo-Tf treatment, the CHO-TRVb-1 cells exceeded basal hepcidin secretion levels at all time-points ($p<0.02$), but it decreased from 30 min to 24 h (1.8-fold; $p<0.01$), unlike the HepG2 cells that maintained constant levels (Fig.4d). Hepcidin levels in CHO TRVb-1 cells were similar to HepG2 cells,

except at 24 h where the CHO TRVb1 cells secreted significantly lower levels than HepG2 cells (1.7-fold; $p<0.02$).

Gene expression analysis: Holo-Tf deprivation in CHO-TRVb1 cells significantly increased *TFRC* expression at 4 h (3.3-fold; $p<0.05$) and significantly reduced s*lc40a1* expression at 2 h ($p<0.03$) and 24 h ($p<0.05$) (Fig.5a). Holo-Tf treatment to CHO TRVb1 cells significantly increased *TFRC* expression at 2 h (3.2-fold; $p<0.03$) and 4 h (5.9-fold; $p<0.05$) (Fig.5b) s*lc40a1* expression was significantly elevated at 2 h (2.2-fold; $p<0.05$) and 4 h (3.4-fold; $p<0.03$), which followed a substantial decrease at 24 h ($p<0.01$). In the HepG2 cells, holo-Tf deprivation caused an insignificant increase in *TFRC* expression (3.6-fold; $p=0.09$) and a significant decrease in *SLC40A1* expression at 24 h ($p<0.03$) (Fig.5c). Following holo-Tf treatment, *TFRC* expression significantly increased at 2 h (3-fold; $p<0.01$) whereas *SLC40A1* expression significantly decreased at 4 h ($p<0.05$) (Fig.5d).

Mitochondrial activity: The CHO TRVb1 and HepG2 cells did not show any major change in mitochondrial activity under holo-Tf deprived and supplemented conditions (Fig.6).

Characterisation of s*lc40a1* in CHO TRVb1-cells

To enable gene expression analyses, the previously unknown sequence of CHO-endogenous s*lc40a1* was partially characterised (Fig.7). These characterised sequences displayed very high percentage similarities with corresponding s*lc40a1* sequences in human (>88%), mouse (>90%) and rat (>90%) (Fig.7b). Partial alignment of the sequence is shown in supplementary Fig.1. The characterised CHO-s*lc40a1* sequence was translated into a protein sequence and compared with ferroportin sequences in other species. Data showed conservation of many functionally significant domains in the proposed transmembrane region and the hepcidin binding region in ferroportin (Fig.7c). Particularly conserved were N144 and V162, which if mutated, exhibit hepcidin insensitivity. The position of C326 in relation to other amino acids is also conserved in the proposed hepcidin binding region, lying outside the transmembrane region and therefore appears to be consistent with its role in binding to hepcidin. K253, Y302 and Y303, which are involved in ferroportin internalisation and degradation upon hepcidin binding are conserved in this characterised CHO-s*lc40a1* sequence and are located in the same position relative to other amino acids as in human, mouse and rat ferroportin [19]. Also, cysteines which form disulphide bonds and usually play a significant role in the folding and stability of proteins [20], are well conserved.

Bioinformatics analysis of hepcidin

Peptide sequence similarities between hamster and other species were assessed. The two predicted hepcidin isoforms in Chinese hamster [21] bear 84 % sequence similarity with each other (Fig.8a) and the terminal 25-mer region bears 84 % sequence similarity with human hepcidin-25 (Fig.8b). Specifically, the first eleven amino acids at its N-terminus are identical to corresponding positions in human hepcidin-25, except that threonine at position 2 in human hepcidin-25 is replaced by serine, which has a side chain similar to threonine. Moreover, there is 100 % conservation of the eight functionally and structurally significant cysteines [22] (Fig.8b).

Discussion

Here, the effect of excess holo-Tf on intracellular iron levels and hepcidin secretion was examined in the CHO TRVb-1 cells that possess iron-unregulated *TFRC* mRNA (*TFRC*ΔIRE) [6] and compared with the HepG2 cells that possess iron-regulated human *TFRC* mRNA. A high concentration of 5 g/L holo-Tf was chosen to promote intracellular iron overload as previous holo-Tf supplementation studies at 2.5 g/L holo-Tf showed no effect on hepcidin mRNA [23] and 30 μM holo-Tf (1.2 g/L) gave conflicting results with either up regulation [24] or down regulation of hepcidin mRNA [25]. On the other hand, when 100 μM holo-Tf (approximately 4 g/L) was used for treatment, an increase in hepcidin mRNA expression was observed [26]. It is also important to note that non-Tf bound iron (NTBI) may play a role in iron uptake. However, pathways for NTBI uptake are less clearly defined compared to TBI uptake. In addition, several previous studies with NTBI showed no effect [1, 24] or even down regulation [15, 25, 27] of hepcidin mRNA. Moreover, the holo-Tf treatment medium was prepared in serum-free Eagle's Minimal Essential Medium (EMEM) that is deprived of inorganic iron sources. This was confirmed by the ferrozine assay, which showed no detectable iron levels in this medium, denoted as 0 g/L (supplementary Fig. 2b), while it showed approximately 6 μM in a FCS (10%)-supplemented EMEM. Thus, the current findings are only based on holo-Tf treatment.

Cellular iron regulation and characterisation of hepcidin response

Human *TFRC* at mRNA and protein levels were confirmed in CHO TRVb-1 cells (Fig.1a and 1b). The cells expressed 2.2-fold higher basal levels of cell-surface TFR1 than HepG2 cells (Fig.1c). Following 5 g/L holo-Tf treatment, the HepG2 cells significantly decreased cell–surface TFR1 expression over time (Fig.3c) and demonstrated an expected iron-regulated

response where *TFRC* transcripts are sensitive to intracellular iron sufficiency due to the IRE region [7] and subsequently decrease cell-surface TFR1 to avoid further iron-uptake, as confirmed here. Contrastingly, the CHO TRVb-1 cells showed constantly elevated expression despite prolonged extracellular holo-Tf excess; a dysregulated characteristic of cell-surface TFR1 in these cells demonstrated in this study for the first time (Fig.3c). This dysregulation due to *TFRC*ΔIRE was also reflected at mRNA level where despite excess extracellular holo-Tf, *TFRC* mRNA expression significantly increased at 2 h and 4 h (Fig.5b).

Although the constitutively high expression of cell-surface TFR1 (Fig.3c) and *TFRC*ΔIRE together indicated a potential for increased iron-uptake, surprisingly, the CHO TRVb-1 cells neither showed higher intracellular iron levels than HepG2 cells under basal conditions (Fig.2a) nor majorly increased iron-uptake upon holo-Tf supplementation (Fig.4b), contrary to the expected. This could be attributed to the elevated *slc40a1* expression, as observed at 2 h of holo-Tf treatment to promote cellular iron-efflux [28] and circumvent any potential increase in iron content caused by increased *TFRC* mRNA expression at the same time (Fig.5b). Accordingly, at 4 h of holo-Tf treatment, a 3.2-fold increase in *slc40a1* expression corresponded to a 2.2-fold decrease in intracellular iron content (Fig.5b and Fig.4b). Such elevations in *slc40a1* expression are consistent with the iron-sensitive feature of the IRE region on *slc40a1* mRNA [29]. This feature prevented cellular iron overload in CHO TRVb-1 cells and did not allow iron levels to exceed beyond that in HepG2 cells, which showed constant levels of *SLC40A1* mRNA expression (Fig.5d).

Interestingly, the CHO TRVb-1 cells are similar to cancer cells that also over-express cell-surface TFR1 to acquire iron for cell survival, growth and proliferation [30]. However, while the human breast cancer cells showed reduced ferroportin expression compared to non-malignant cells [31], presumably to retain intracellular iron, the CHO TRVb-1 cells differed and showed elevated *slc40a1* expression, aiming for iron-efflux (Fig.5). Thus, unlike cancer cells, the CHO-TRVb1 cells exhibited a fascinating regulatory phenomenon where *scl40a1* maintained intracellular iron-homeostasis in presence of excess extracellular holo-Tf and abundant cell-surface TFR1, while *TFRC* mRNA was incapable of contributing to intracellular iron-sensing due to *TFRC*ΔIRE. The overall aim of protecting the cells from excess-iron-mediated toxicity was achieved, as confirmed through the MTT assay, which showed no signs of cell toxicity (Fig.6).

Here, we presented novel data where the CHO TRVb-1 cells secreted hepcidin under basal conditions; and following holo-Tf treatment, exceeded basal levels at all time-points (Fig.2b and Fig.4d). This resembled the human response to excess systemic iron levels [1] and suggested that these cells were suitable to study holo-Tf-induced hepcidin responses. The antibody utilised detects the N-terminal 14 amino acid region of human hepcidin-25 [12], (Fig. 8b, amino acids in bold). Here, 12 out of the total 14 amino acids are identical to the corresponding region in hamster hepcidin (Fig. 8b, highlighted grey). Moreover, in position-2 of human hepcidin-25, threonine in human is replaced by a structurally and functionally similar amino acid serine in hamster. This leaves only one dissimilar amino acid at position 12. Such high level of similarity in the antibody binding region of hepcidin-25 fully supports the successful detection of hamster hepcidin by this method. The method used here has also been successfully used to detect hepcidin in rhesus monkeys [32].

Under basal conditions, the CHO TRVb-1 cells secreted significantly lower levels of hepcidin than HepG2 cells (Fig.2b). Since HepG2 cells are of hepatic origin whereas CHO TRVb-1 cells are ovary-derived, this data is consistence with the tissue–specific nature of hepcidin, where, in human and animals, hepcidin is predominantly secreted by liver hepatocytes with lower amounts being secreted by other tissues [33], however the peptide expression level has been reported higher in rat kidney than human kidney by immunoblot analysis (Kulaksiz et al., 2005). Also, overexpressed TFR1 expression on the cell-surface may have disturbed its physiological ratio with HFE and TFR2, the hepcidin inducing proteins [34], thereby causing lower hepcidin secretion under basal conditions. However, upon holo-Tf treatment, hepcidin levels in CHO TRVb-1 cells matched the levels in HepG2 cells, at least up to 4 h (Fig.4d), which indicated that tissue-specificity was overruled and hepcidin response to holo-Tf treatment governed. This may have occurred via two mechanisms; first, upon binding of holo-Tf to TFR1, the TFR1-bound HFE may be displaced and free to bind to TFR2 to induce hepcidin [3] and second, due to the predominance of response–specific factors over tissue-specific factors [35]. Since, the expected intracellular iron overload was not achieved, exactly how and to what extent intracellular iron levels modulate hepcidin secretion remains to be elucidated.

Characterisation of CHO-*slc40a1* and bioinformatics study of hepcidin peptide sequences

In order to study iron-efflux in CHO TRVb-1 cells and cellular iron regulation via real-time PCR, genomic similarities between species were examined (supplementary Table 1) and partial characterisation of the previously unknown *slc40a1* sequence in CHO TRVb-1 cells was achieved (Fig.7a and 7b). As expected, the characterised s*lc40a1* sequences in CHO TRVb-1 cells bore more than 88 % sequence similarities with the corresponding sequences of human, mouse and rat (Table 1) and were subsequently used to design primers for gene expression analysis (Supplementary Fig.1, Fig.5a and 5b). Comparison of the characterised and then translated CHO-*slco40a1* sequence with ferroportin sequences from other species showed an overall 92 % similarity. Several amino acids in the functionally significant domains such as the proposed transmembrane region and hepcidin binding region are conserved, as presented here for the first time (Fig.7c). Overall, the data indicates that the sequence of ferroportin is well conserved amongst species.

The two hepcidin isoforms of Chinese hamster [21] show high sequence similarity with human hepcidin-25 (Fig.8b). This is particularly in the N-terminal region that is important for its interaction with ferroportin, the furin cleavage site on prohepcidin that releases bioactive hepcidin and the 8 cysteine residues, which are believed to have structural and functional significance [22].

Conclusion

Despite the substantially higher levels of cell-surface TFR1, intracellular iron overload was not achieved in CHO TRVb-1 cells, possibly due to elevated *slc40a1* expression. This demonstrated the importance of the iron–efflux protein ferroportin in maintaining intracellular iron homeostasis in the absence of iron-regulated *TFRC* mRNA. Furthermore, we have demonstrated novel data whereby CHO-endogenous hepcidin secretion occurred under basal conditions and was further stimulated upon 5 g/L holo-Tf stimulus, resembling the human response to iron treatment.

Acknowledgements: Prof. Rob Evans for assistance with the urea gel assay.

Financial support: #Dr Kosha Mehta was supported by a scholarship from the University of Westminster.

Conflict of interest: Kosha Mehta, Pamela Greenwell, Derek Renshaw, Mark Busbridge, Mitla Garcia, Sebastien Farnaud and Vinood B. Patel declare that they have no conflict of interest.

Compliance with Ethical Requirements: This article does not contain any studies conducted on human or animal subjects.

Abbreviations:

CHO	Chinese hamster ovary
EMEM	Eagle's minimal essential medium
H	Hours
IRE	Iron responsive element
IRP	Iron regulatory protein
Min	minutes
MTT	3-(4,5-Dimethylthiazol-2-yl)-2,5-diphenyltetrazolium bromide
PCR	Polymerase chain reaction
Sec	Seconds
Slc40a1	Gene encoding the iron-exporter protein ferroportin
Tf	Transferrin
TFR	Transferrin receptor
TFRC	Gene encoding the iron-importer protein transferrin receptor 1

References

1 Pigeon, C., Ilyin, G., Courselaud, B., Leroyer, P., Turlin, B., Brissot, P. and Loreal, O. (2001) A new mouse liver-specific gene, encoding a protein homologous to human antimicrobial peptide hepcidin, is overexpressed during iron overload. J Biol Chem. **276**, 7811-7819

2 Preza, G. C., Pinon, R., Ganz, T. and Nemeth, E. (2013) Cellular catabolism of the iron-regulatory peptide hormone hepcidin. PLoS One. **8**, e58934

3 Schmidt, P. J., Toran, P. T., Giannetti, A. M., Bjorkman, P. J. and Andrews, N. C. (2008) The transferrin receptor modulates Hfe-dependent regulation of hepcidin expression. Cell Metab. **7**, 205-214

4 Farnaud, S., Rapisarda, C., Bui, T., Drake, A., Cammack, R. and Evans, R. W. (2008) Identification of an iron-hepcidin complex. Biochem J. **413**, 553-557

5 Kanamori, Y., Murakami, M., Matsui, T. and Funaba, M. (2014) Hepcidin expression in liver cells: evaluation of mRNA levels and transcriptional regulation. Gene. **546**, 50-55

6 McGraw, T. E., Greenfield, L. and Maxfield, F. R. (1987) Functional expression of the human transferrin receptor cDNA in Chinese hamster ovary cells deficient in endogenous transferrin receptor. ed.)^eds.). pp. 207-214

7 Casey, J. L., Hentze, M. W., Koeller, D. M., Caughman, S. W., Rouault, T. A., Klausner, R. D. and Harford, J. B. (1988) Iron-responsive elements: regulatory RNA sequences that control mRNA levels and translation. Science. **240**, 924-928

8 Evans, R. W. and Williams, J. (1978) Studies of the binding of different iron donors to human serum transferrin and isolation of iron-binding fragments from the N- and C-terminal regions of the protein. Biochem J. **173**, 543-552

9 Riemer, J., Hoepken, H. H., Czerwinska, H., Robinson, S. R. and Dringen, R. (2004) Colorimetric ferrozine-based assay for the quantitation of iron in cultured cells. Anal Biochem. **331**, 370-375

10 Rosignoli, G., Lim, C. H., Bower, M., Gotch, F. and Imami, N. (2009) Programmed death (PD)-1 molecule and its ligand PD-L1 distribution among memory CD4 and CD8 T cell subsets in human immunodeficiency virus-1-infected individuals. Clin Exp Immunol. **157**, 90-97

11 Pepper, S. E., Borkowski, M., Richmann, M. K. and Reed, D. T. (2010) Determination of ferrous and ferric iron in aqueous biological solutions. Anal Chim Acta. **663**, 172-177

12 Busbridge, M., Griffiths, C., Ashby, D., Gale, D., Jayantha, A., Sanwaiya, A. and Chapman, R. S. (2009) Development of a novel immunoassay for the iron regulatory peptide hepcidin. Br J Biomed Sci. **66**, 150-157

13 Mosmann, T. (1983) Rapid colorimetric assay for cellular growth and survival: application to proliferation and cytotoxicity assays. J Immunol Methods. **65**, 55-63

14 Bahr, S. M., Borgschulte, T., Kayser, K. J. and Lin, N. (2009) Using microarray technology to select housekeeping genes in Chinese hamster ovary cells. Biotechnol Bioeng. **104**, 1041-1046

15 Jacolot, S., Ferec, C. and Mura, C. (2008) Iron responses in hepatic, intestinal and macrophage/monocyte cell lines under different culture conditions. Blood Cells Mol Dis. **41**, 100-108

16 Livak, K. J. and Schmittgen, T. D. (2001) Analysis of relative gene expression data using real-time quantitative PCR and the 2(-Delta Delta C(T)) Method. Methods. **25**, 402-408

17 Maniatis, T. S., Joseph & Fritsch, E. F. (Edward F.) (1982) Molecular cloning : a laboratory manual,. Cold Spring Harbor Laboratory, Cold Spring Harbor, N.Y

18 Turkewitz, A. P., Amatruda, J. F., Borhani, D., Harrison, S. C. and Schwartz, A. L. (1988) A high yield purification of the human transferrin receptor and properties of its major extracellular fragment. J Biol Chem. **263**, 8318-8325

19 Wallace, D. F., Harris, J. M. and Subramaniam, V. N. (2009) Functional analysis and theoretical modeling of ferroportin reveals clustering of mutations according to phenotype. Am J Physiol Cell Physiol. **298**, C75-84

20 Sevier, C. S. and Kaiser, C. A. (2002) Formation and transfer of disulphide bonds in living cells. Nat Rev Mol Cell Biol. **3**, 836-847

21 Pruitt, K. D., Brown, G. R., Hiatt, S. M., Thibaud-Nissen, F., Astashyn, A., Ermolaeva, O., Farrell, C. M., Hart, J., Landrum, M. J., McGarvey, K. M., Murphy, M. R., O'Leary, N. A., Pujar, S., Rajput, B., Rangwala, S. H., Riddick, L. D., Shkeda, A., Sun, H., Tamez, P., Tully, R. E., Wallin, C., Webb, D., Weber, J., Wu, W., DiCuccio, M., Kitts, P., Maglott, D. R., Murphy, T. D. and Ostell, J. M. (2014) RefSeq: an update on mammalian reference sequences. Nucleic Acids Res. **42**, D756-763
22 Clark, R. J., Tan, C. C., Preza, G. C., Nemeth, E., Ganz, T. and Craik, D. J. (2011) Understanding the structure/activity relationships of the iron regulatory peptide hepcidin. Chem Biol. **18**, 336-343
23 Gehrke, S. G., Kulaksiz, H., Herrmann, T., Riedel, H. D., Bents, K., Veltkamp, C. and Stremmel, W. (2003) Expression of hepcidin in hereditary hemochromatosis: evidence for a regulation in response to the serum transferrin saturation and to non-transferrin-bound iron. Blood. **102**, 371-376
24 Lin, L., Valore, E. V., Nemeth, E., Goodnough, J. B., Gabayan, V. and Ganz, T. (2007) Iron transferrin regulates hepcidin synthesis in primary hepatocyte culture through hemojuvelin and BMP2/4. Blood. **110**, 2182-2189
25 Nemeth, E., Valore, E. V., Territo, M., Schiller, G., Lichtenstein, A. and Ganz, T. (2003) Hepcidin, a putative mediator of anemia of inflammation, is a type II acute-phase protein. Blood. **101**, 2461-2463
26 Rapisarda, C., Puppi, J., Hughes, R. D., Dhawan, A., Farnaud, S., Evans, R. W. and Sharp, P. A. (2010) Transferrin receptor 2 is crucial for iron sensing in human hepatocytes. Am J Physiol Gastrointest Liver Physiol. **299**, G778-783
27 Dzikaite, V., Holmstrom, P., Stal, P., Eckes, K., Hagen, K., Eggertsen, G., Gafvels, M., Melefors, O. and Hultcrantz, R. (2006) Regulatory effects of tumor necrosis factor-alpha and interleukin-6 on HAMP expression in iron loaded rat hepatocytes. J Hepatol. **44**, 544-551
28 McKie, A. T., Marciani, P., Rolfs, A., Brennan, K., Wehr, K., Barrow, D., Miret, S., Bomford, A., Peters, T. J., Farzaneh, F., Hediger, M. A., Hentze, M. W. and Simpson, R. J. (2000) A novel duodenal iron-regulated transporter, IREG1, implicated in the basolateral transfer of iron to the circulation. Mol Cell. **5**, 299-309
29 Muckenthaler, M. U., Galy, B. and Hentze, M. W. (2008) Systemic iron homeostasis and the iron-responsive element/iron-regulatory protein (IRE/IRP) regulatory network. Annu Rev Nutr. **28**, 197-213
30 Kuvibidila, S., Gauthier, T., Warrier, R. P. and Rayford, W. (2004) Increased levels of serum transferrin receptor and serum transferrin receptor/log ferritin ratios in men with prostate cancer and the implications for body-iron stores. J Lab Clin Med. **144**, 176-182
31 Pinnix, Z. K., Miller, L. D., Wang, W., D'Agostino, R., Jr., Kute, T., Willingham, M. C., Hatcher, H., Tesfay, L., Sui, G., Di, X., Torti, S. V. and Torti, F. M. (2010) Ferroportin and iron regulation in breast cancer progression and prognosis. Sci Transl Med. **2**, 43ra56
32 Coe, C. L., Lubach, G. R., Busbridge, M. and Chapman, R. S. (2013) Optimal iron fortification of maternal diet during pregnancy and nursing for investigating and preventing iron deficiency in young rhesus monkeys. Res Vet Sci. **94**, 549-554
33 Park, C. H., Valore, E. V., Waring, A. J. and Ganz, T. (2001) Hepcidin, a Urinary Antimicrobial Peptide Synthesized in the Liver. J Biol Chem. ed.)^eds.). pp. 7806-7810
34 D'Alessio, F., Hentze, M. W. and Muckenthaler, M. U. (2012) The hemochromatosis proteins HFE, TfR2, and HJV form a membrane-associated protein complex for hepcidin regulation. J Hepatol. **57**, 1052-1060
35 Truksa, J., Lee, P. and Beutler, E. (2009) Two BMP responsive elements, STAT, and bZIP/HNF4/COUP motifs of the hepcidin promoter are critical for BMP, SMAD1, and HJV responsiveness. Blood. **113**, 688-695

Figure captions

Fig.1 *TFRC* transcripts and protein in CHO-TRVb-1 cells

Fig.2 Iron and hepcidin levels in CHO TRVb-1 cells under basal conditions

Fig.3 Cell-surface TFR1 in CHO-TRVb-1 cells following iron treatment

Fig.4 Iron and hepcidin levels in CHO TRVb-1 cells following iron treatment
Fig.5 mRNA expression of human *TFRC* and endogenous *slc40a1* in CHO TRVb-1 cells
Fig.6 Mitochondrial activity in CHO TRVb-1 cells following iron treatment
Fig.7 Characterisation of *slc40a1* in CHO TRVb-1 cells
Fig.8 Alignments of human and hamster hepcidin

Figure Legends

Fig.1 *TFRC* transcripts and TFR1 protein in CHO TRVb-1 cells

(a): The cDNA from CHO TRVb-1 and Wt CHO cells was amplified and run on 1 % agarose gel. Lane 1= Amplicon of Wt CHO cDNA obtained by using CHO-endogenous *TfRC* primers; expected product-size is 230 bp; lane 2= PCR of Wt CHO cDNA with human *TFRC* primers; no product expected; lane 3= PCR of CHO TRVb-1 cDNA with CHO-endogenous *TfRC* primers; no product expected; lane 4= Amplicon of CHO TRVb-1 cDNA obtained by using human *TFRC* primers; expected product size is 179 bp.

(b): Cell pellet of CHO TRVb-1 cells was probed with human TFR1 antibody and Western blot detected human TFR1 protein in CHO TRVb-1 cells. Lane 1= CHO TRVb-1 cells in non-reducing conditions; lane 2= CHO TRVb-1 cells in reducing conditions.

(c): Cell-surface TFR1 levels in CHO TRVb-1 cells and HepG2 cells were assessed. Data is presented as mean ± SEM (n=3). *$p<0.01$ compared to HepG2 cells (1-way ANOVA).

Fig.2 Basal levels of iron and hepcidin peptide secretion in CHO TRVb-1 cells

Intracellular iron levels (a) and hepcidin secretion (b) in CHO TRVb-1 cells were measured by using the ferrozine assay and radioimmunoassay, respectively, under basal conditions. Data is presented as mean ± SEM (n=3). *$p<0.05$ and **$p<0.01$ compared to 30 min in CHO TRVb-1 cells; $^{\#}p<0.04$ and $^{\#\#}p<0.02$ compared to HepG2 cells at 30 min and 24 h, respectively (2-way ANOVA). Analysis showed significant differences between cell-types ($p=0.019$) and for cell-type x time ($p=0.039$) (post-hoc analysis by Tukey's method)

Fig. 3 Effect of iron supplementation on cell-surface expression of TFR1 in CHO TRVb-1 cells

CHO TRVb-1 and HepG2 cells were treated with 5 g/L holo-Tf and cell-surface TFR1 was assessed by flow cytometry. Representative images of CHO TRVb-1 cells following treatment for 24 h and 48 h are depicted in 'a' and 'b', respectively. Data is presented as mean ± SEM (n=3). *$p <0.01$ compared to 24 hours in HepG2 cells (1-way ANOVA).

Fig.4 Effect of iron supplementation on intracellular iron levels and hepcidin secretion in CHO TRVb-1 cells

Intracellular iron levels (a & b) and hepcidin secretion (c & d) in CHO TRVb-1 cells were measured by using the ferrozine assay and radioimmunoassay, respectively. Data is presented

as mean ± SEM (n=3). *p<0.01 compared to 30 min in CHO TRVb-1 cells; #p<0.02 compared to HepG2 cells at the corresponding time-point; ^p<0.05 compared to 4 h in CHO TRVb-1 cells (1-way ANOVA).

Fig.5 Gene expression studies in CHO TRVb-1 and HepG2 cells

mRNA expression levels of human *TFRC* and endogenous *slc40a1* in CHO TRVb-1 cells upon holo-Tf deprivation (0 g/L) (a) and holo-Tf supplementation (b) are shown. Also, the effect of holo-Tf deprivation (c) and holo-Tf supplementation (d) in HepG2 cells has been shown. Data is presented as mean ± SEM (n=3). *p<0.05, **p<0.03 compared to 30 min; #p<0.01 compared to 4 h (1-way ANOVA).

Fig.6 Effect of iron supplementation on mitochondrial activity in CHO TRVb-1 cells

CHO TRVb-1 and HepG2 cells were treated with 0 g/L (a) and 5 g/L (b) holo-Tf and mitochondrial activity in the cells was determined by using the MTT assay. Data is presented as mean ± SEM (n=3).

Fig.7 Characterisation of CHO-endogenous *slc40a1*

(a): Amplicons of *slc40a1* in CHO TRVb-1 cells and rodents with primers (F1) and (R1) in the first round of sequencing have been shown. Here, lane 1= rat liver DNA (control), lane 2= mouse kidney cDNA (control), expected sizes of controls were 160 bp. Lane 3= CHO TRVb-1 DNA, Lane 4= negative control. Encircled product in lane 3 was purified and its sequence identity was confirmed as described in the methods section.

(b): The table shows percentage sequence similarities between the characterised CHO-*slc40a1* sequences and *slc40a1* sequences of related species.

(c): The alignment underpins functional study of the characterised CHO- *slc40a1* sequence. The characterised sequence was translated using the functional tool "*TRANSLATE*" available at *web.expasy.org*, and compared with ferroportin sequences of different species.

Key to alignment:

- **Proposed transmembrane region**
- ***Proposed hepcidin binding domain***
- **K253,Y302,Y303: amino acids affecting ferroportin degradation and internalisation**
- **N144H, V162 Δ: Mutations that disruption ferroportin function**
- *** represents conserved amino acid between species**

Fig.8 Conservation of hepcidin sequence amongst species

Conservation of amino acids between the predicted preprohepcidin sequences in Chinese hamster (*Cricetulus griseus)* (a) and between hepcidin isoforms in hamster and hepcidin in human (b) are shown. Downward arrow shows the cleavage-site of furin convertase, which releases bioactive hepcidin.

Characterisation of hepcidin response to holotransferrin treatment in CHO TRVb-1 cells

Figures

Figure 1

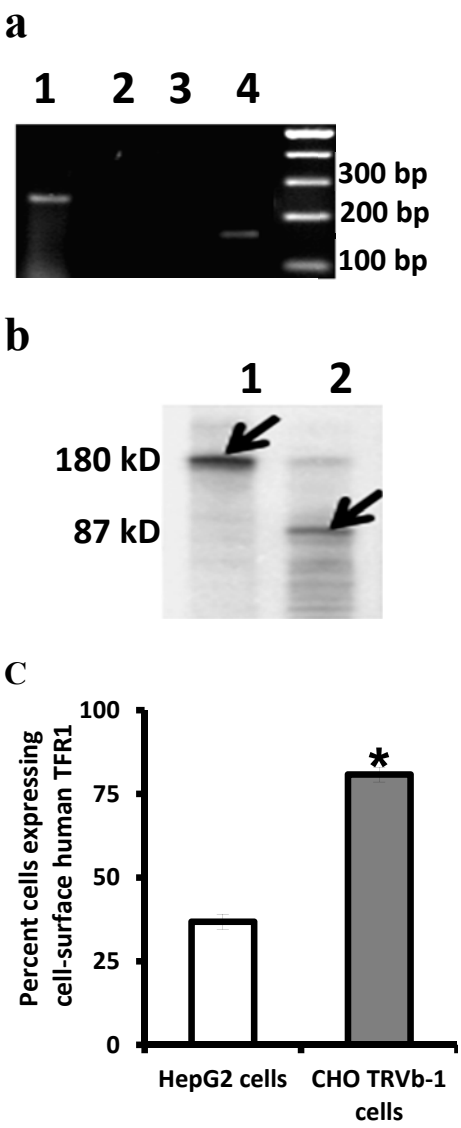

Figure 2

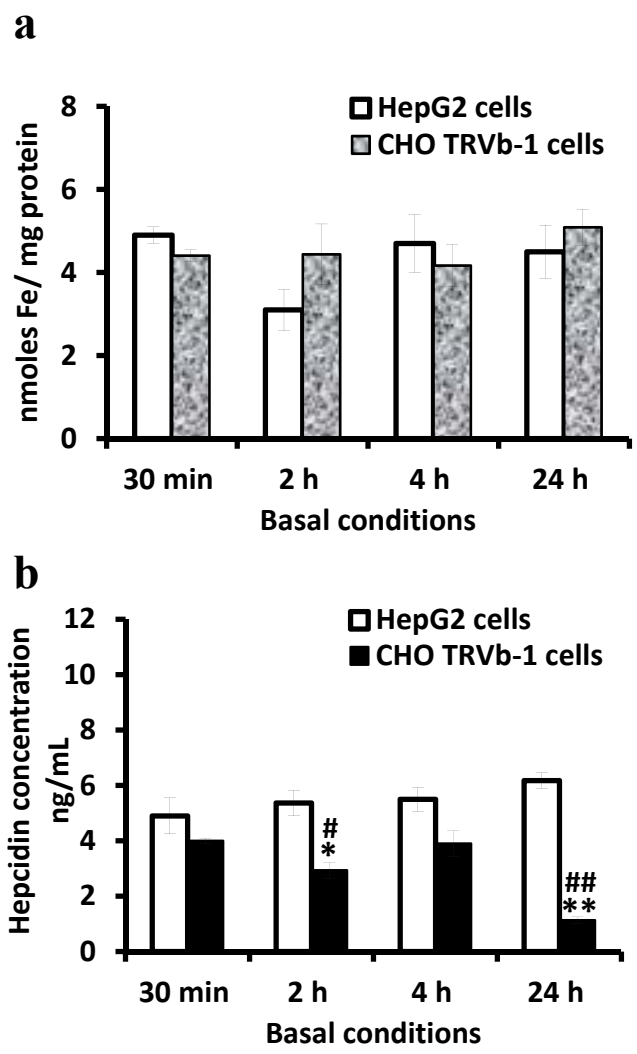
a
HepG2 cells
CHO TRVb-1 cells
nmoles Fe/ mg protein
8
6
4
2
0
30 min
2 h
4 h
24 h
Basal conditions
b
HepG2 cells
CHO TRVb-1 cells
Hepcidin concentration ng/mL
12
10
8
6
4
2
0
#
*
##
**
30 min
2 h
4 h
24 h
Basal conditions

Figure 3

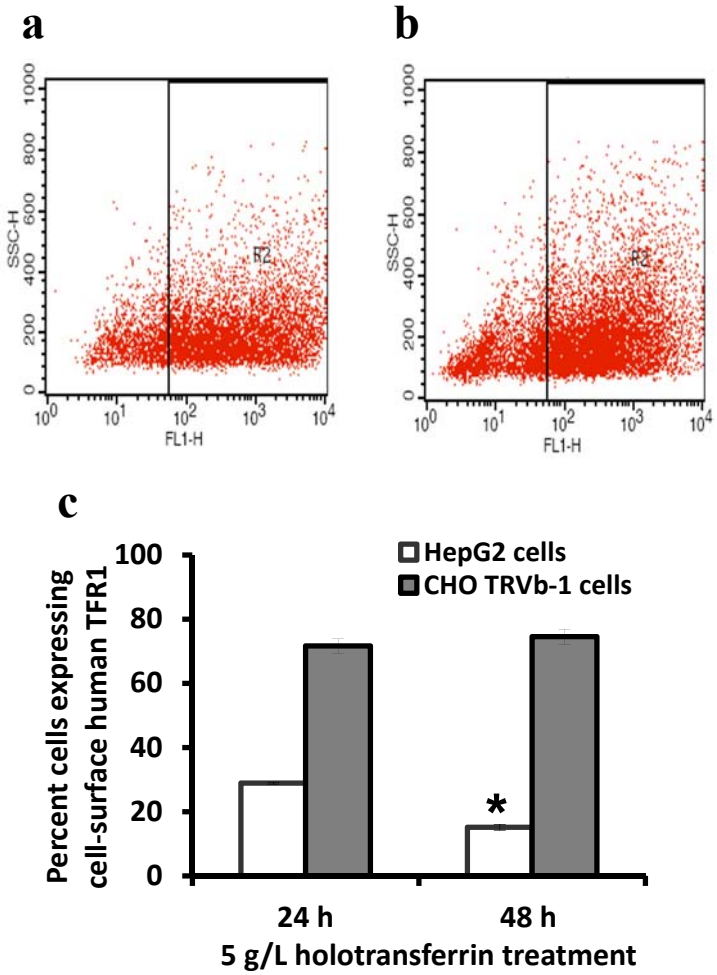
a
b
SSC-H
FL1-H
R2
c
Percent cells expressing cell-surface human TFR1
HepG2 cells
CHO TRVb-1 cells
*
24 h
48 h
5 g/L holotransferrin treatment

Figure 4

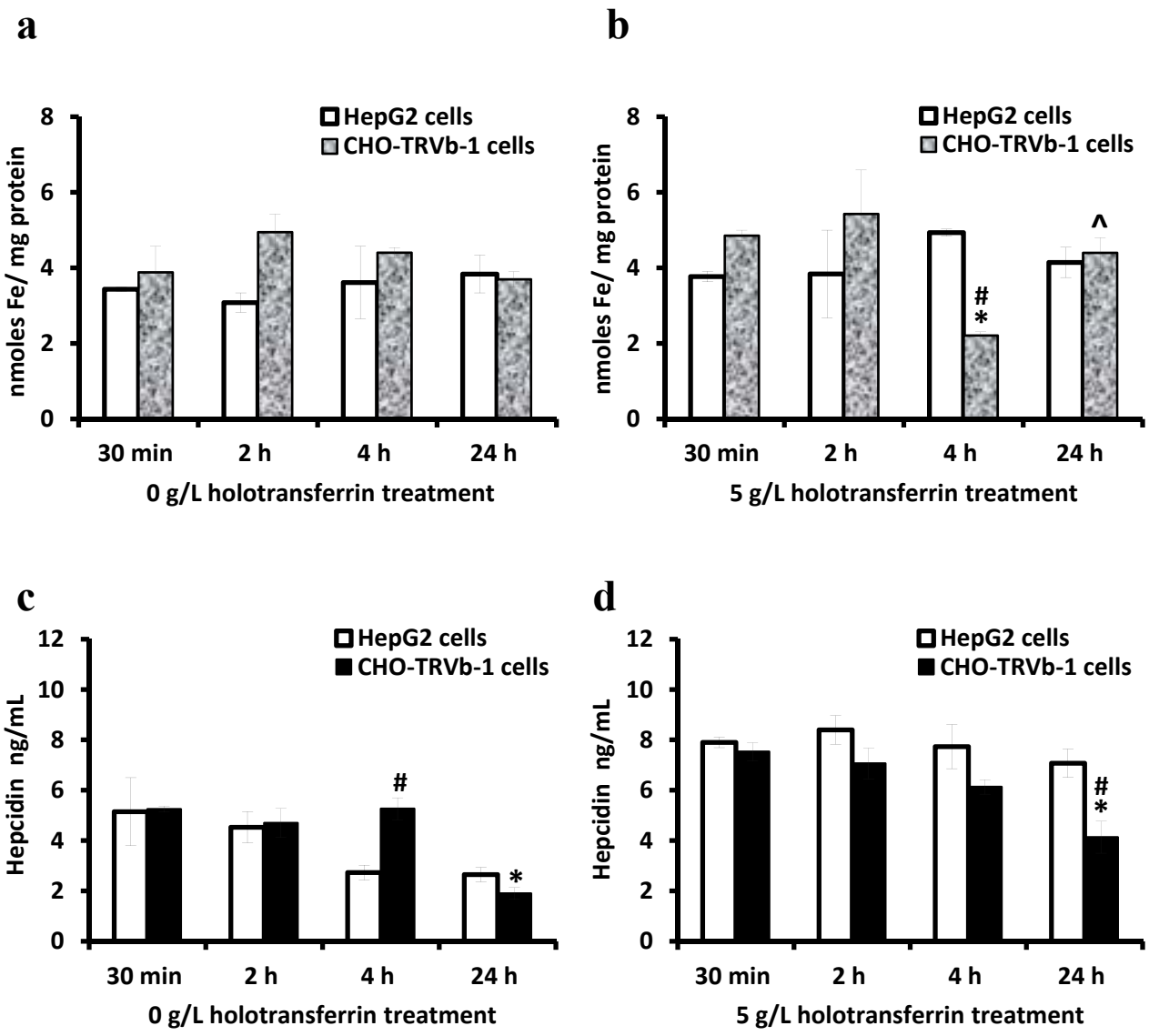
a
b
c
d
HepG2 cells
CHO-TRVb-1 cells
nmoles Fe/ mg protein
Hepcidin ng/mL
30 min
2 h
4 h
24 h
0 g/L holotransferrin treatment
5 g/L holotransferrin treatment
#
*
^

Figure 5

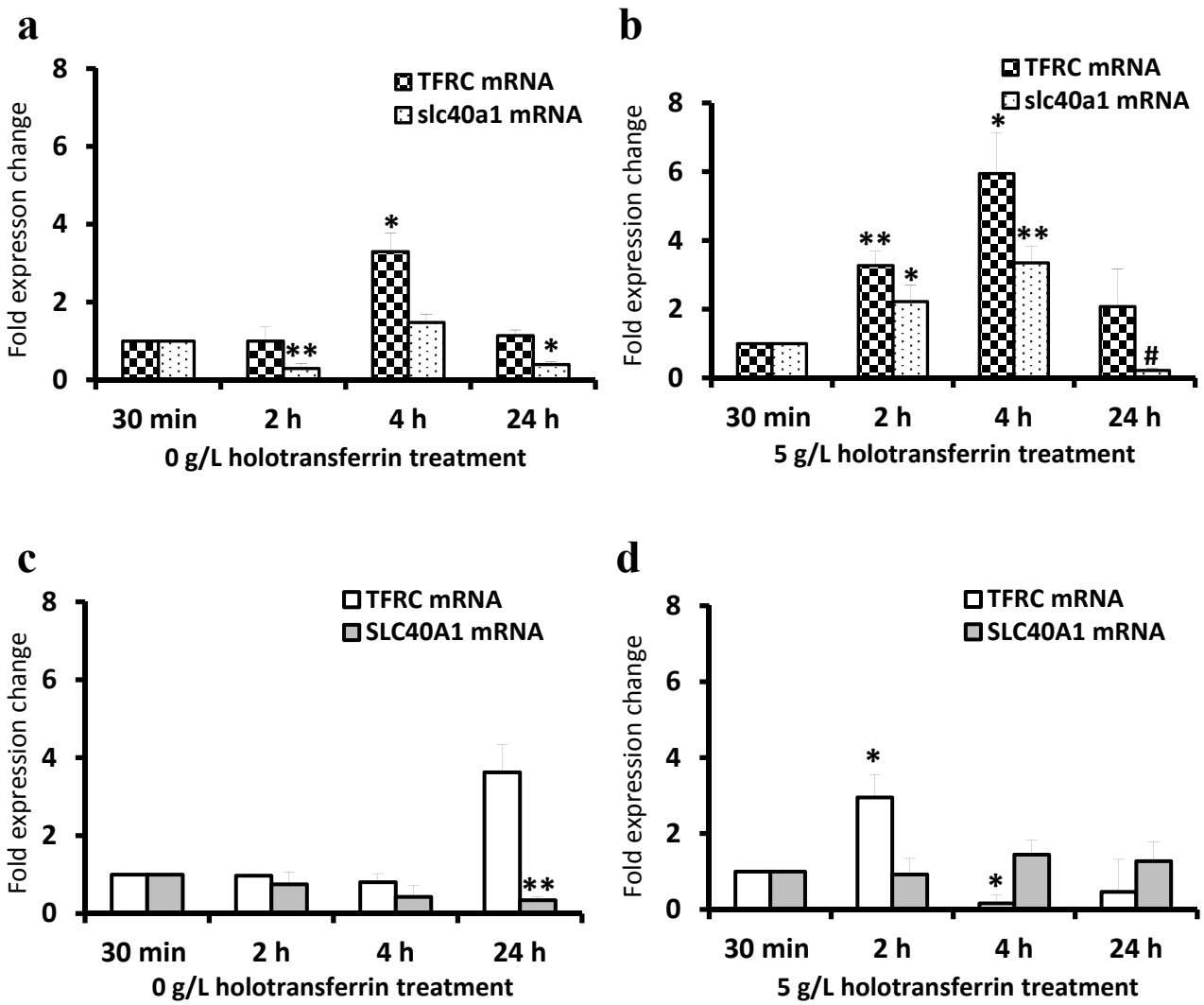
a
TFRC mRNA
slc40a1 mRNA
Fold expresson change
0 g/L holotransferrin treatment
30 min
2 h
4 h
24 h
b
TFRC mRNA
slc40a1 mRNA
Fold expression change
5 g/L holotransferrin treatment
c
TFRC mRNA
SLC40A1 mRNA
Fold expression change
0 g/L holotransferrin treatment
d
TFRC mRNA
SLC40A1 mRNA
Fold expression change
5 g/L holotransferrin treatment

Figure 6

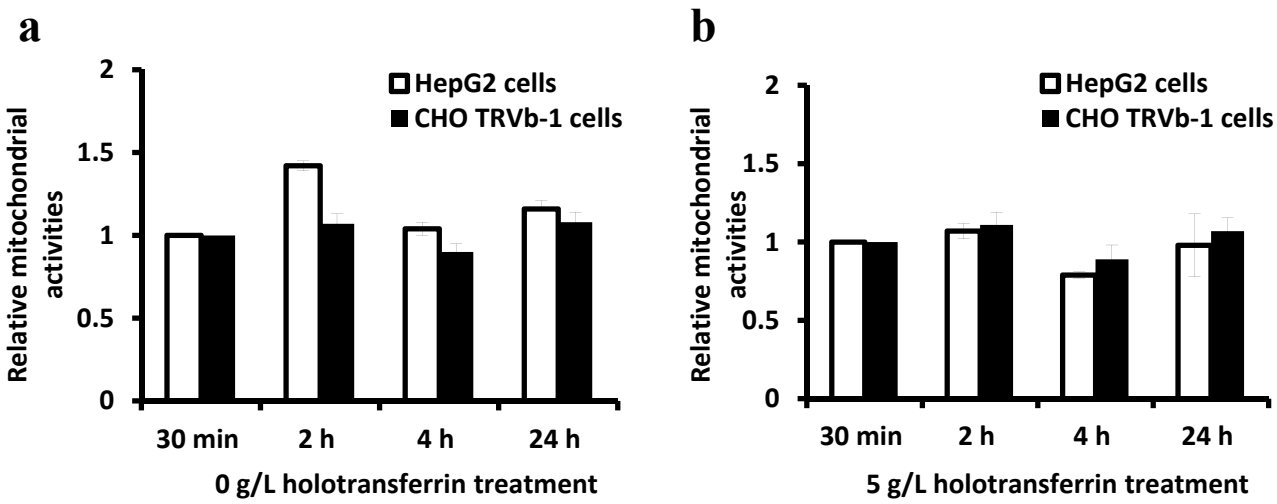
a
b
HepG2 cells
CHO TRVb-1 cells
Relative mitochondrial activities
2
1.5
1
0.5
0
30 min
2 h
4 h
24 h
0 g/L holotransferrin treatment
5 g/L holotransferrin treatment

Figure 7

a

b

Species	First round of sequencing	Second round of sequencing
Human	92 %	89 %
Mouse	92 %	93 %
Rat	96 %	92 %

C

```
Human      MTRAGDHNRQRGCCGSLADYLTSAKFLLYLGHSLSTWGDRMWHFAVSVFLVELYGNSLLL 60
Mouse      ------------------------------------------------------------
Rat        MTKSRDQTHQEGCCGSLANYLTSAKFLLYLGHSLSTWGDRMWHFAVSVFLVELYGNGLLL 60
Hamster    -----------------------------------------------------SLLL 4

Human      TAVYGLVVAGSVLVLGAIIGDWVDKNARLKVAQTSLVVQNVSVILCGIILMMVFLHKHEL 120
Mouse      TAVYGLVVAGSVLVLGAIIGDWVDKNARLKVAQTSLVVQNVSVILCGIILMMVFLHKNEL 60
Rat        TAVYGLVVAGSVLVLGAIIGDWVDKNARLKVAQTSLVVQNVSVILCGIILMMVFLHKNEL 120
Hamster    TAVYGLVVAGSVLVA----------------QTSLVVQNVSVILCGIILMMVFLHKNEL 47
           ************                    ************************:**

Human      LTMYHGWVLTSCYILIITIANIANLASTATAITIQRDWIVVVAGEDRSKLANMNATIRRI 180
Mouse      LTMYHGWVLTVCYILIITIANIANLASTATAITIQRDWIVVVAGENRSRLADMNATIRRI 120
Rat        LNMYHGWVLTVCYILIITIANIANLASTATAITIQRDWIVVVAGENRSRLADMNATIRRI 180
Hamster    LTMYHGWVLTVCYILIITIANIANLASTATAITIQRDWIVVVAGENRSRLADMNATIRRI 107
           *.******** ************************************:**:**:********
                                N144H                V162Δ

Human      DQLTNILAPMAVGQIMTFGSPVIGCGFISGWNLVSMCVEYVLLWKVYQKTPALAVKAGLK 240
Mouse      DQLTNILAPMAVGQIMTFGSPVIGCGFISGWNLVSMCVEYFLLWKVYQKTPALAVKAALK 180
Rat        DQLTNILAPMAVGQIMTFGSPVIGCGFISGWNLVSMCVEYFLLWKVYQKTPALAVKAALK 240
Hamster    DQLTNILAPMAVGQIMTFGSPVIGCGFISGWNLVSMCVEYFLLWKVYQKTPALAVKAVLK 167
           ************************************.**************** **

Human      EEETELKQLNLHKDTEPKPLEGTHLMGVKDSNIHELEHEQEPTCASQMAEPFRTFRDGWV 300
Mouse      VEESELKQLTSPKDTEPKPLEGTHLMGEKDSNIRELECEQEPTCASQMAEPFRTFRDGWV 240
Rat        VEESELKQLTSPKDTEPKPLEGTHLMGEKDSNIRELECEQEPTCASQIAEPFRTFRDGWV 300
Hamster    VEEAELKQLNLPKDTEPKSLEGTHLMGEKDSNIRELEHEQESTCASQIAEPFRTFRDGWV 227
           **:*****.  ******.******** *****:*** ***.*****:************
                      K253

Human      SYYNQPVFLAGMGLAFLYMTVLGFDCITTGYAYTQGLSGSILSILMGASAITGIMGTVAF 360
Mouse      SYYNQPVFLAGMGLAFLYMTVLGFDCITTGYAYTQGLSGSILSILMGASAITGIMGTVAF 300
Rat        SYYNQPVFLAGMGLAFLYMTVLGFDCITTGYAYTQGLSGSILSVLMGASAITGIMGTVAF 360
Hamster    SYYNQPVFLAGMGLAFLYMTVLGFDCITTGYAYTQGLS---------------------- 265
           ****************************************
            Y302,Y303              C326
```

Figure 8

a

```
Hamster Hepc-1 MAQSTKIQAACLLLLLIAPQLLRAATEGTRVRQPEALQPQHRTADQTDRTDRTLLIPKRT
Hamster Hepc 2 MAQSTKIQAACLLLLLIASLA-SSTLLQQLVRQPEALQPQHRTKAQTDRTDRTLLIPKRT
               ******************     ::     *************  ***************

Hamster Hepc-1 KRDSHFPICIFCCYCCGNFKCGVCCKT 87
Hamster Hepc-2 KRDSHFPICIFCCYCCGNFKCGVCCKT 86
               **************************
```

b